Effect of Multi-Component Transport Model on Soot Prediction in Opposed-Jet Ethylene Diffusion Flames

Anders Borg[1,2], Harry Lehtiniemi[1], and Fabian Mauss[3]
[1]Lund Combustion Engineering - LOGE AB
Lund, Sweden
[2]Chalmers University of Technology
Gothenburg, Sweden
[3]Brandenburg University of Technology — BTU
Cottbus, Germany

1   Introduction

The prediction of soot from hydrocarbon combustion is a challenging problem that involves a number of theoretical principles in chemistry and physics. The influence of gas-phase transport property modeling on soot prediction was recently investigated by Zimmer et al. [1]. Their investigations concerning transport properties were limited to a study of the differences between unity Lewis number and mixture-averaged transport, where they confirmed a strain-dependent effect. In this paper, we aim to investigate the differences in soot predictions when using a detailed multi-component transport model instead of a mixture-average transport model. H radicals are known to be sensitive on soot growth [2]. We therefore want to understand, if the mixture average diffusion approximation is accurate enough to predict the influence of radical diffusion from the inner layer at stoichiometric conditions to the soot growth layer at fuel rich conditions. The impact of multi-component diffusion on phenomena other than soot formation and growth is quite striking, as noted for example by Brown and Revzan [3] who reported the transport coefficients to be of equal sensitivity as chemical reaction rates when modeling laminar premixed flames. With these two studies in mind, a clear effect of the transport model on the soot prediction is therefore expected. In this paper two ethylene/air counter-flow flames of Wang et al. [4] will be used to investigate the impact of multicomponent diffusion on soot prediction.

2   Computational model

The calculation of one-dimensional counter-flow flames is performed using the commercial software *LOGEsoft* [5]. Potential flow boundary conditions and axial symmetry are specified in accordance with the calculations presented in [4]. Radiation of soot, CO_2 and H_2O is considered in the calculation. The

chemical reaction mechanism is taken from Mauss [6]. It is suitable for C_1-C_3 combustion, it includes pathways for polycyclic aromatic hydrocarbon (PAH) growth, and it contains 82 species and 806 reactions including backward reactions.

The soot model is the same as in [6], where it is described in further detail. Here only a brief account of the model will be given. The first soot particle is formed through the coagulation of two planar PAH molecules, a process referred to as *particle inception*. This process defines the smallest soot particle, which is considered to be in solid phase. PAH larger than four aromatic rings are allowed to combine and incept the first soot particle. PAH larger than four aromatic rings are also allowed to coagulate with soot particles. This process is called *condensation* and leads to the increase of soot mass. When soot particles collide, they can combine to larger spherical particle or to agglomerates in a process called *coagulation*. The agglomerate structure affects the soot surface available for surface reactions. The model accounts for the agglomerate structure by assuming a constant fractal dimension for soot, $D_f = 1.8$. The heterogeneous *surface growth* reactions are modeled following the hydrogen-abstraction-acetylene-addition (HACA) mechanism [7] with a separate ring closure (HACARC) [6]. The process where an acetylene molecule is abstracted from the soot surface is referred to as *fragmentation* [6]. Soot is oxidized through heterogeneous reactions with molecular oxygen and hydroxyl radicals, which is simply called *oxidation*. The evolution of the soot particle size distribution function is solved using the method of moments [7]. In this study 3 moments are solved. The zeroth moment (M_0) gives the number of soot particles and the first moment (M_1) gives the total soot mass. The second moment (M_2) does not have a direct physical interpretation, but holds information of the skewness of the size distribution function and can be used together with M_0 and M_1 to obtain the variance of the size distribution function. The transport equations for the moments (M_0-M_2) include particle size dependent diffusion coefficients, as well as a size independent term for thermophoresis [8]. The latter term is dependent on the gas phase viscosity.

Two approaches for transport coefficient evaluation are used and compared with respect to their influence on soot formation in this work. The first and simplified model is referred to as *mixture-averaged*. In the mixture-averaged scheme the diffusion is evaluated using an effective binary diffusion coefficient, as in [9]. Since this approximation can give a net diffusive mass flow, the correction by Jones and Boris is also utilized [10]. The thermal conductivity and viscosity used in this scheme are calculated with an empirical formula derived by Mathur et al. [11]. The thermal diffusion coefficient is evaluated from the mixture-average diffusion coefficient and a thermal diffusion ratio, calculated as described by Paul and Warnatz [12]. This approach is today in use by the most laminar flame predicting software.

The second and detailed model, is called *multi-component*. Multi-component transport means that a detailed model based on the Chapman-Enskog solution of Maxwell-Boltzmann's transport equation is employed. An introduction to the theory can be found in the book of Chapman and Cowling [13]. The exact equation systems used in the present work to obtain multi-component transport properties are taken from Ern and Giovangigli [14]. Their derivation relies on an extension by Waldmann and Trübenbacher [15] to a gas with several species, of the Wang-Chang and Uhlenbeck theory [16] for a single species gas that includes vibration and rotational energy. In the implementation used in this study, the calculation of collision integrals for the Stockmayer potential uses the Monchick and Mason tabulation procedure [17]. For the ratios of collision integrals appearing in the equation systems of Ern and Giovangigli, the functional approximations contained in their work is used. The so-called combination rules for obtaining potential parameters for pairs of molecules from the single molecule parameters is taken from the paper of Mason and Monchich [18]. For the temperature dependence of the collision number the expression derived by Brau and Jonkman [19], which is an extension of the work of Parker [20], is used. The linear equation systems of Ern and Giovangigli, corresponding to a full number of basis functions are solved using direct numerical calculation techniques, without using the approximation strategy for computational speed-up utilized by Ern and Giovangigli. This provides a more accurate calculation of diffusion, thermal

diffusion and heat conductivity, bypassing the extra work to analyze any eventual error arising from the reduced basis and the approximate calculation method.

3   Results and Discussion

In table 1 the computational results obtained with the mixture-average and multi-component model is compared to the experimental and computational results of Wang et al. [4]. Only two of the flames (flames 1 and 3) were investigated in this paper because of the lack of velocity data. It is seen that the numerical and experimental values are in good agreement for both transport models. The calculations with the mixture-averaged transport model result in approximately 15% higher soot concentrations compared to the calculations with the multi-component transport model. The multi-component calculation fits the experimental values worse for flame 1 than the mixture-average calculation, while the opposite is true for flame 3. It should be kept in mind that the uncertainty in the experiment and modelling parameters is probably much greater than the differences between the models for these flames. The shapes of the soot volume fraction profiles match the experiments with good precision, as can be seen in the right panel of figure 1 and 2, for flames 1 and 3 respectively. The calculated soot volume fraction of Wang et al. is considerably flatter, a result of their calculations not considering condensation of PAH molecules on the soot surface. When condensation was used their model also showed a sharper profile that compared more favorable to the experimental results, which they also noted.
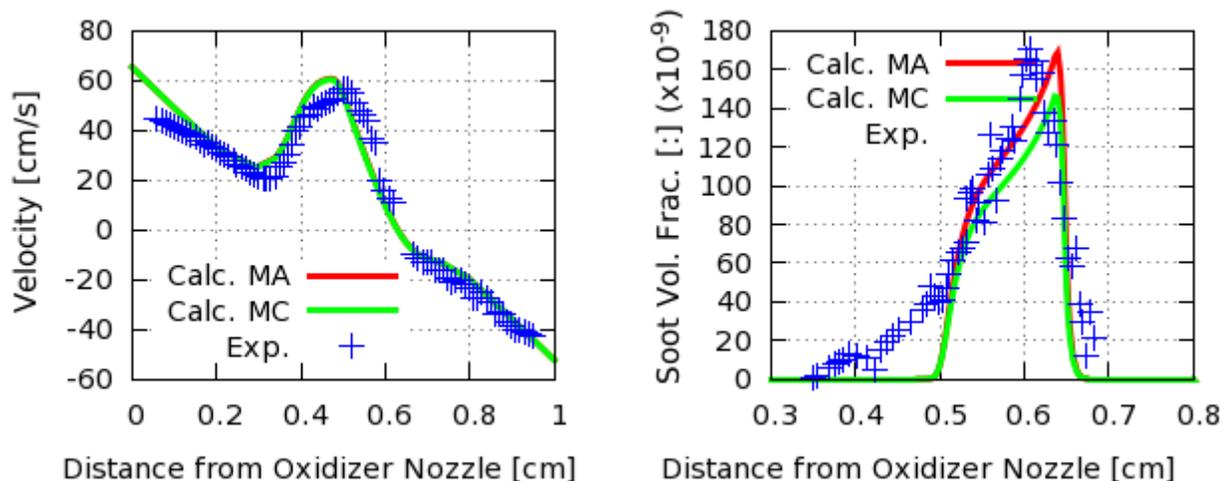

Figure 1. (Left) Experimental velocities for flame 1 of Ref. [4] compared to calculated results obtained with mixture-average (MA) and multi-component transport model (MC). (Right) Soot volume fraction comparison for the same cases.

The velocity boundary values for flame 1 and 3 were taken directly from the numerical calculation data of [4]. For both flames there is a slight offset towards the fuel side in the calculated soot volume fraction profile. It seems likely that a better velocity matching, specifically performed for the chemical mechanism used for our calculations, will improve the fits for these flames.

Table 1: Comparison of experiments and calculations from Ref. [4] to the calculations in this paper

Flame	Exp. Fv Ref. [4]	Calc. Fv Ref. [4]	Calc. Fv (Mix. Avg)	Calc. Fv (Mult.-comp.)
1	1.7E-7	1.4E-7	1.7E-7	1.5E-7
3	2.4E-7	1.6E-7	3.2E-7	2.8E-7

The maximum temperature obtained for both flames in the present calculation is approximately 100 K higher than what was obtained in [4], possibly resulting from differences in the different chemical reaction mechanisms. The mole fraction of acetylene, which is around 6 % in the calculation presented in [4], is approximately a factor 2 smaller in the present calculation also due to reaction mechanism differences.
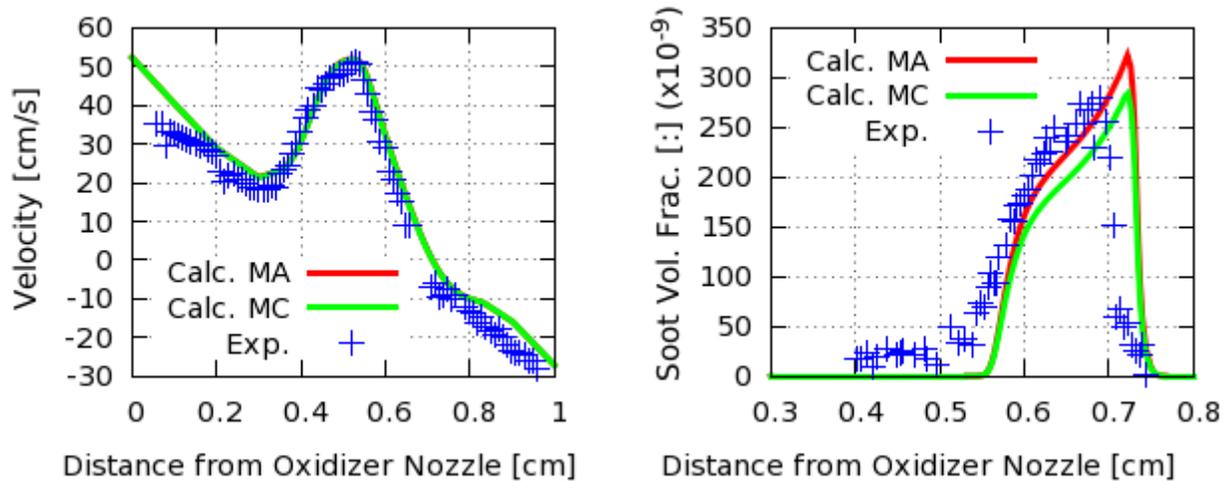

Figure 2. (Left) Experimental velocities for flame 3 in Ref. [4] compared to results obtained with mixture-average (MA) and multi-component transport model (MC). (Right) Soot volume fraction comparison for the same cases.

The method for transport property calculation is not affecting M_0 (number density) as can be seen in the left panel in figure 3. It is very similar for both the mixture-average and the multi-component transport model, for both flames 1 and 3. The right panel of figure 3 shows M_1, where the effect of the transport model is clearly seen. The transport model affects both flames in the same way. M_2, not shown, shows a very similar behavior as M_1. Figures showing a detailed analysis of the effect of each transport process, i.e. heat conductivity, viscosity, thermal and ordinary diffusion, will unfortunately not fit in the present extended abstract. The effect of the different transport processes will therefore be shortly mentioned only. Taking the mixture-averaged diffusion model as a reference, turning on the multi-component calculation for the diffusion flux will decrease the predicted soot volume fraction. Turning on the multi-component calculation for the heat conductivity, rather than the diffusion flux, will decrease the soot volume fraction by a greater amount as a result of a very slight change in temperature (approximately 10 K). The multi-component calculation for viscosity will decrease the soot volume fraction very slightly compared to a mixture-average calculation. The multi-component calculation of heat conductivity has for the investigated flames a higher sensitivity on the soot volume fraction than any other multi-component transport process.
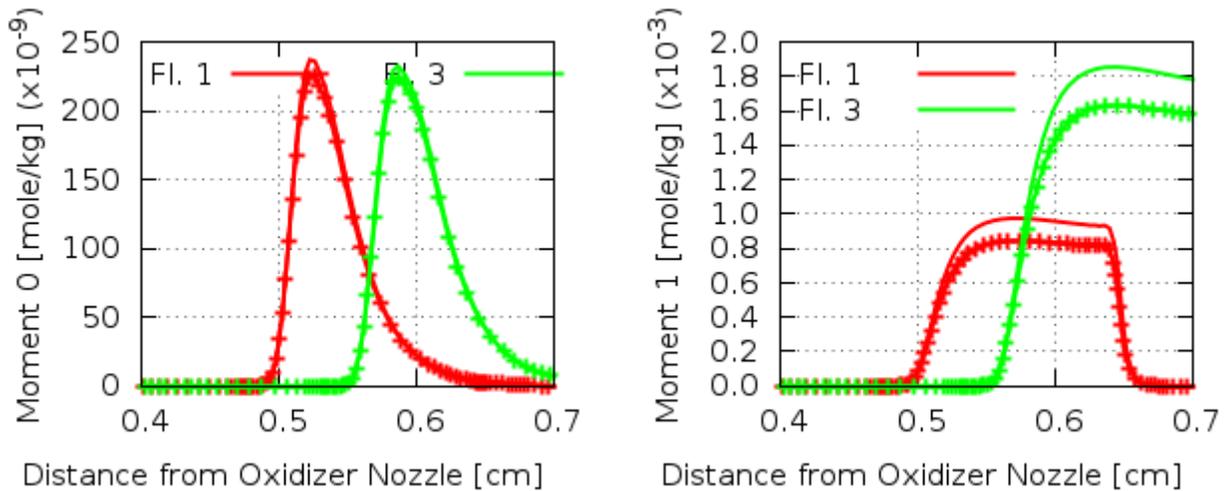
Figure 3. Calculated soot moment 0 (Left) and soot moment 1 (Right) of flames 1 and 3. Dashed lines indicate multi-component calculation while solid lines show mixture-averaged calculation.

4 Conclusions

Soot calculations were performed for a laminar ethylene counter-flow flame configuration using 1-D flame modeling. A detailed soot model was used with two different models for gas-phase transport. The calculations showed good agreement compared to the soot experiments of [4], both in absolute values and in the shape of the soot profile. The mixture-averaged transport models predicted approximately 15 percent more soot (in terms of soot volume fraction) compared to the multi-component transport model, with no corresponding change in soot number density. The heat conductivity was the most sensitive of the transport processes for soot prediction. Heat conductivity decreased the total soot amount when using multi-component transport. The second largest sensitivity was due to the diffusion, which also decreased the soot amount with the multi-component transport model, although to a lesser degree. Smallest sensitivity to the soot volume fraction was found to be the viscosity, which only lowered the soot volume fraction very slightly. The viscosity effects can be related to thermophoresis, heat conductivity affects temperature and chemical reactions, while diffusion coefficients affect surface growth by radical transport to the soot growth layer. Other experiments might result in a different sensitivity of the species transport coefficients.

References

[1] Zimmer L, Pereira FM, van Oijen JA, de Goey LPH (2016). Investigation of mass and energy coupling between soot particles and gas species in modelling ethylene counterflow diffusion flames. Combust Theor Model, doi 10.1080/13647830.2016.1238512.

[2] Mauss, F, Schäfer, T, and Bockhorn, H, (1994) Inception and Growth of Soot Particles in Dependence on the Surrounding Gas Phase, Combust Flame 99:697-705.

[3] Brown NJ, Revzan KL (2005). Comparative sensitivity analysis of transport properties and reaction rate coefficients. Int J Chemical Kinet 37:538.

[4] Wang H, Du DX, Sung CJ, Law CK (1996). Experiments and numerical simulation on soot formation in opposed-jet ethylene diffusion flames. Proc Combust Inst 26:2359-2368.

[5] LOGEsoft, www.loge.se.

[6] Mauss F (1998). Entwicklung eines kinetischen Modells der Rußbildung mit schneller Polymerisation, RWTH Aachen (ISBN 3-89712-152-2).

[7] Frenklach M, Wang H (1990). Detailed modeling of soot particle nucleation and growth. Proc Combust Inst 23:1559–1566.

[8] Mauss, F., Trilken, B., Breitbach, H., and Peters, N., (1994) Soot Formation in Partially Premixed Diffusion Flames at Atmospheric Pressure, in, H. Bockhorn (Ed.), Soot Formation in Combustion–Mechanism and Models, Springer Verlag.

[9] Hirschfelder JO, Curtiss CF (1949). Theory of propagation of flames Part I: General Equations. Third Symposium on Combustion and Flame and Explosion Phenomena. 121.

[10] Oran ES, Boris JP (1981). Detailed modeling of combustion systems. Prog Energ Combust 7:1-72.

[11] Mathur S, Tondon PK, Saxena SC (1967). Heat conductivity in ternary gas mixtures. Mol Phys 12:569.

[12] Paul P, Warnatz J (1998). A re-evaluation of the means used to calculate transport properties of reacting flows. Proc Combust Inst 27:495.

[13] Chapman S, Cowling TG. (1970). The mathematical theory of non-uniform gases. Cambridge University Press.

[14] Ern A, Giovangigli V (2014). Multicomponent Transport Algorithms. Springer Berlin.

[15] Waldmann L, Trübenbacher E. (1962). Formale Kinetische Theorie von Gasgemischen aus anregbaren Molekülen. Z Naturforsch A 17:363.

[16] Wang-Chang CS, Uhlenbeck GE. (1951). Transport Phenomena in Polyatomic Gases. University of Michigan Publications.

[17] Monchick L, Mason EA. (1961). Transport Properties of Polar Gases. J Chem Phys 35:1676.

[18] Mason EA, Monchick L. (1962). Transport Properties of Polar-Gas Mixtures. J Chem Phys 36:2746.

[19] Brau CA., Jonkman RM. (1970). Classical Theory of Rotational Relaxation in Diatomic Gases. J Chem Phys 52:477.

[20] Parker JG. (1959). Rotational and Vibrational Relaxation in Diatomic Gases. Phys Fluids 2:449.